N-alkylated oligoamide α-helical proteomimetics

ARTICLE *in* ORGANIC & BIOMOLECULAR CHEMISTRY · MAY 2010

Impact Factor: 3.56 · DOI: 10.1039/c001164a · Source: PubMed

Organic & Biomolecular Chemistry

www.rsc.org/obc

Volume 8 | Number 10 | 21 May 2010 | Pages 2269–2480

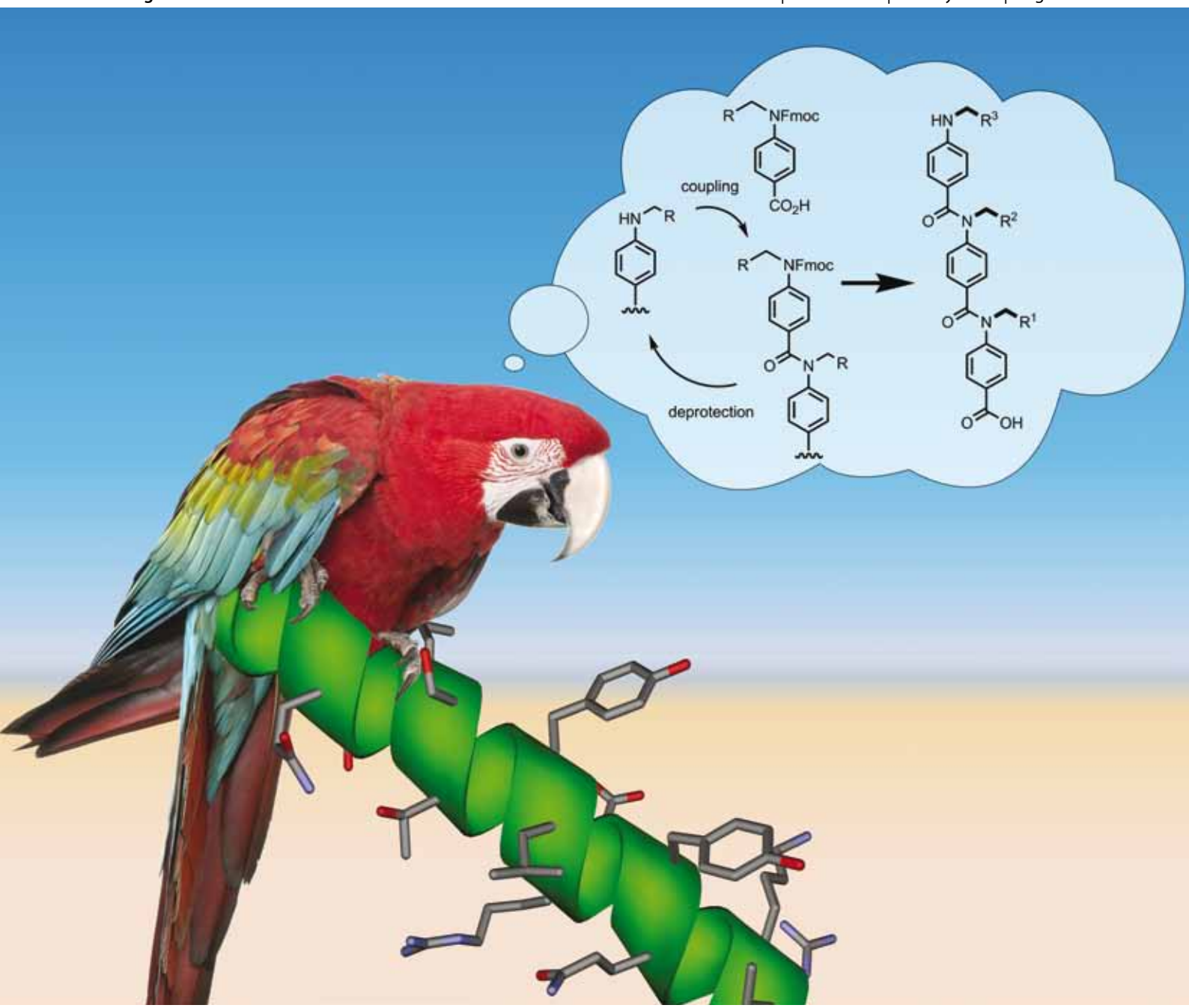

ISSN 1477-0520

RSC Publishing

FULL PAPER
Andrew J. Wilson *et al.*
N-Alkylated oligoamide α-helical proteomimetics

COMMUNICATION
Marcel Jaspers *et al.*
Dermacozines, a new phenazine family from deep-sea dermacocci Isolated from a Mariana Trench sediment

N-alkylated oligoamide α-helical proteomimetics†

Frederick Campbell,[a] Jeffrey P. Plante,[a] Thomas A. Edwards,*[b] Stuart L. Warriner*[a] and Andrew J. Wilson*[a]

Received 18th January 2010, Accepted 5th March 2010
First published as an Advance Article on the web 18th March 2010
DOI: 10.1039/c001164a

Generic approaches for the design and synthesis of small molecule inhibitors of protein–protein interactions (PPIs) represent a key objective in modern chemical biology. Within this context, the α-helix mediated PPIs have received considerable attention as targets for inhibition using small molecules, foldamers and proteomimetics. This manuscript describes a novel *N*-alkylated aromatic oligoamide proteomimetic scaffold and its solid-phase synthesis—the first time such an approach has been used for proteomimetics. The utility of these scaffolds as proteomimetics is exemplified through the identification of potent μM inhibitors of the p53–*h*DM2 helix mediated PPI—a key oncogenic target.

Introduction

The elaboration of generic approaches for competitive inhibition of protein–protein interactions (PPIs) is recognised as a major goal of contemporary chemical biology.[1–4] The challenge arises from the difficulty in designing ligands that can mimic a natural protein partner; covering a large surface area of the target protein, and matching the diverse and discontinuous non-covalent interactions made at the protein–protein interface. For the α-helix mediated class of PPI[5] in which an α-helix from one protein binds to a complementary cleft on its protein partner (*e.g.* Bcl-2 family[6,7] and p53-*h*DM2[8–10] interactions) such a general approach is starting to emerge. In addition to the various small molecule inhibitors of the Bcl-2 family[7,11–14] and p53–hDM2[9,15–18] interactions, oligomers that mimic the spatial and compositional presentation of α-amino acid side chains made by the interacting helix have been identified. In the first approach, β-peptides,[19–21] mixed α/β peptides[22–24] and other foldamers[25–31] closely mimic both the core helical structure and side chain presentation found within the helical motif whilst offering modular solid phase syntheses. *Proteomimetic*[32] scaffolds[32–50] first introduced by the Hamilton group, mimic only the side chain presentation that is key to protein surface recognition; however, robust methods for generation of screening libraries are less well defined.[47,49,50] Amongst the *proteomimetic* scaffolds, aromatic oligoamides[51] are attractive as inhibitors[34,45,47,48,52] of α-helix mediated PPIs because they exhibit predictable folding patterns controlled largely by the preferred conformation of the aryl–NHCO–aryl bond and adjacent *ortho* interactions. Such oligomers represent a natural bridge between β-peptides and α-helix *proteomimetics* but solid-phase library syntheses for generation of screening libraries have not been described. In the current manuscript we introduce one of the simplest proteomimetic scaffolds described to date, outline its solid phase synthesis and illustrate its use as a platform for the discovery of potent inhibitors of the p53–*h*DM2 interaction.

Results and discussion

We recently described the synthesis and cyclisation of *N*-alkylated aromatic oligoamides[53,54] facilitated by the preferred *cis* geometry[55] first observed by Shudo and co-workers[56] for *N*-alkylated aromatic oligoamides/ureas. We observed that in an extended conformation, the *N*-alkyl substituents mimic the side chain presentation of functionality made by the *i*, *i* + 4 and *i* + 7 (8) side chains of an α-helix. Encouraged by Rebek's[57] observations that self-assembled capsules can revert the intrinsic preference for the *cis* amide conformer through non-covalent interaction with the *trans* form, we reasoned that *N*-alkylated trimers might similarly adopt the desired extended conformation and inhibit α-helix mediated PPIs. Fig. 1 shows a model of the helix mimetic in an extended conformation and a comparison with the α-helix of the p53 peptide from the crystal structure of p53–*h*DM2 (here the p53 peptide makes key contacts from Phe 19, Trp 23 and Leu 26 to the cleft on *h*DM2).[8]

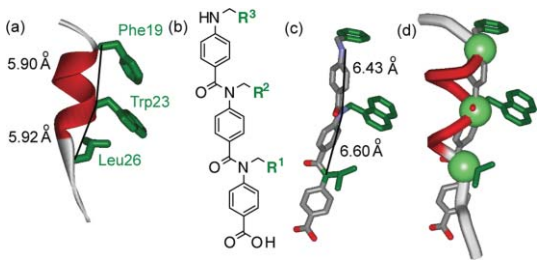

Fig. 1 (a) *h*DM2 binding p53 helix illustrating the spatial position of key *h*DM2 binding side chains; (b) structure of an *N*-alkylated aromatic oligoamide helix mimetic; (c) molecular model (MMFFs force field) of an aromatic oligoamide mimic of the p53 sequence illustrating reasonable reproduction of the spatial positioning of helix side chains in the *i*, *i* + 4 and *i* + 7 positions (d) overlay of the helix mimetic and p53 peptide (RMSD is 0.493 (Å) for α-carbons of helix and nitrogens of mimetic).

Synthesis

We were keen to develop a solid phase synthesis of the aromatic oligoamides that would facilitate library synthesis. Basing the synthetic strategy on Fmoc protection of the aniline would also

[a]*School of Chemistry, University of Leeds, Woodhouse Lane, Leeds, LS2 9JT, United Kingdom. E-mail: A.J.Wilson@leeds.ac.uk, S.L.Warriner@leeds.ac.uk; Fax: +44 (0)113 3436565; Tel: +44 (0)113 3431409*
[b]*Astbury Centre for Structural Molecular Biology, University of Leeds, Woodhouse Lane, Leeds, LS2 9JT, United Kingdom. E-mail: T.A.Edwards@leeds.ac.uk*

† Electronic supplementary information (ESI) available: Synthetic procedures, protein expression, binding studies and HSQC data. See DOI: 10.1039/c001164a

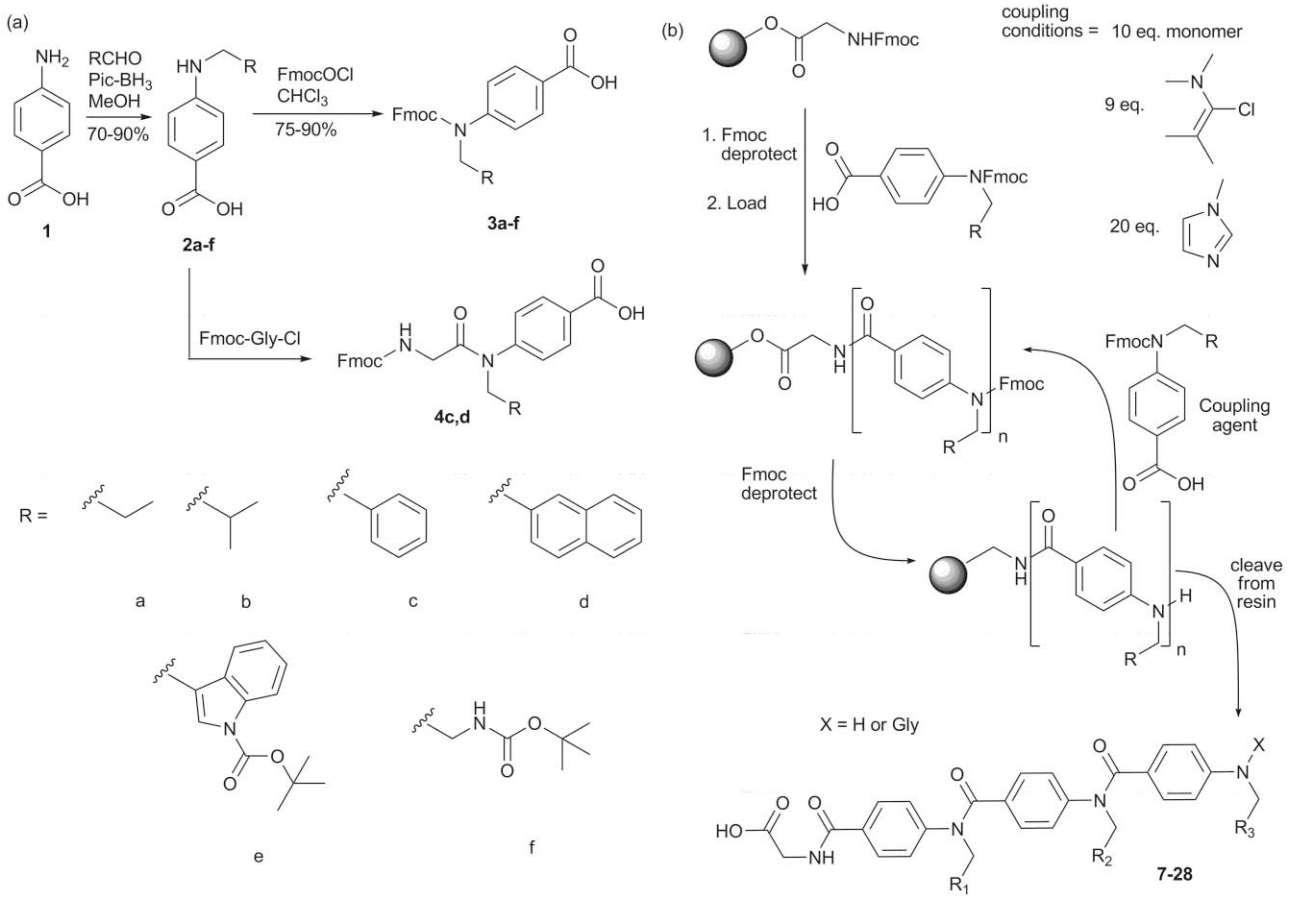

Scheme 1 (a) Synthesis of Fmoc protected *N*-alkylated *p*-aminobenzoic acid monomers **3** and **4**, and (b) outline of procedure used for solid-phase synthesis of *N*-alkylated aromatic oligoamide α-helix mimetics.

enable standard side chain protection from classical peptide synthesis to be used and make the mimetic syntheses compatible with existing solid support chemistries. Our synthetic approach for solid-phase synthesis builds on prior studies by Kilbinger and co-workers.[58] Initial studies linked the protected aminobenzoic acids **3a–f** (Scheme 1a) directly to a Wang resin support using 1-(mesitylene-2-sulfonyl)-3-nitro-1,2,4-triazole (MSNT) promoted coupling.[59] Although this method was effective at forming a C-terminal ester, we found it challenging to monitor the efficiency of subsequent coupling steps *i.e.* due to the water sensitivity of the coupling chemistries explored during this study (see below) it was challenging to ascertain if loading, coupling or resin cleavage was the source of poor levels of dimer formation. We therefore constructed all the oligomers on preloaded Gly-Wang resin to remove uncertainties associated with initial resin loading, generating a robust amide bond in both loading and coupling reaction (Gly was selected to avoid any side chain contribution to binding in our subsequent analysis: see binding studies). Our earlier studies on the coupling of amino benzoic acid derivatives[48,53,54,60] relied upon *in situ* generation of the acid chloride at elevated temperatures. Such a method is not compatible with the manual solid-phase synthesis developed in this study. Therefore, in order to effect efficient couplings at room temperature, we reacted Ghosez's α-chloroenamine reagent[61] with the monomer in chloroform for ~3 h prior to addition of *N*-methylimidazole (MeIm) as base and then transferred the mixture onto the resin (Scheme 1b). Due to the water sensitivity of the coupling reagent, and low reactivity of the aniline towards acid chlorides at room temperature, this required significant care to exclude water from the coupling reaction. We tested a range of other coupling reagents including PyBOP, HCTU, TFFH and dichlorotriphenylphosphorane none of which effected the transformation at room temperature whilst coupling also failed when the base was diisopropylethylamine. In the small library we constructed for this investigation, we employed a 10-fold excess of monomer, 9-fold excess of coupling reagent and 20-fold excess of base relative to the maximum resin loading. We found coupling efficiencies under these conditions to be >95%. Following cleavage from the resin using TFA, final compounds were generally obtained by precipitation in high purity (>95% by LC-MS). Of the monomers we attempted to couple, only the indole functionalized monomer was problematic—we found that the side chain was cleaved from the scaffold during resin cleavage, presumably due to acid mediated elimination. However, the method is clearly compatible with conventional protecting group strategies and chemistry developed for solid phase peptide synthesis as tBoc protected monomer **3f** coupled smoothly. We also synthesized trimers functionalized at the N-terminus with glycine on the basis that this might improve solubility due to the higher pK_a of the primary amine as compared to the secondary aniline. Direct coupling of Fmoc glycine to the N-terminus of our

trimers failed; this was solved by use of Fmoc-Gly functionalized monomers **4c** and **d** (see ESI†) in the final coupling step.

Binding studies

Once we established our method, a small library of compounds (**7–28**) was assembled for screening against the p53–*h*DM2 interaction (Fig. 2). Compounds **5** and **6** from our earlier work on macrocyclizations were also added to the library. The library compounds were screened at 10 μM in a single point fluorescence anisotropy competition assay for inhibition of the p53–*h*DM2 interaction.[21,38,48] Briefly, a short p53 peptide labelled with fluorescein undergoes an increase in anisotropy upon titration with *h*DM2. Upon addition of inhibitor and perturbation of the equilibrium, this signal then decreases again and the resultant anisotropy values are used to calculate a % inhibition. Our small library gave a full range of inhibition values. It was also possible to pick out some simple structure affinity relationships from this experiment. For instance, the most potent inhibitors had side chain sequences similar in nature to the key Phe 19, Trp23, Leu 26, side chains of the p53 peptide (*e.g.* R^3 = Ph, R^2 = Nap, R^1 = ^{i}Pr **15** and R^3 = ^{i}Pr, R^2 = Ph, R^1 = Ph **12**). Oligomers with only two side chains *e.g.* **7** were poor inhibitors indicating a requirement for trimeric motifs for successful inhibition, and suggesting that potent compounds unfold and adopt the desired extended conformation. We also found tentative evidence to suggest that dipole alignment is unimportant as compounds with reversed sequences were equipotent (*e.g.* R^1 = Ph, R^2 = Ph, R^3 = ^{i}Pr **12** and R^1 = ^{i}Pr, R^2 = Ph, R^3 = Ph **11**) whilst the requirement for hydrophobic aromatic side chains is also evidenced by the much poorer potency of **8** and **9**. Curiously, the oligomers capped with glycine at the N-terminus (**17–28**) all exhibited poor potency (and contrary to our expectations, solubility). Presumably, the protonated N-terminus makes a repulsive electrostatic contact with the protein reducing potency relative to those compounds without a glycine at the N-terminus.

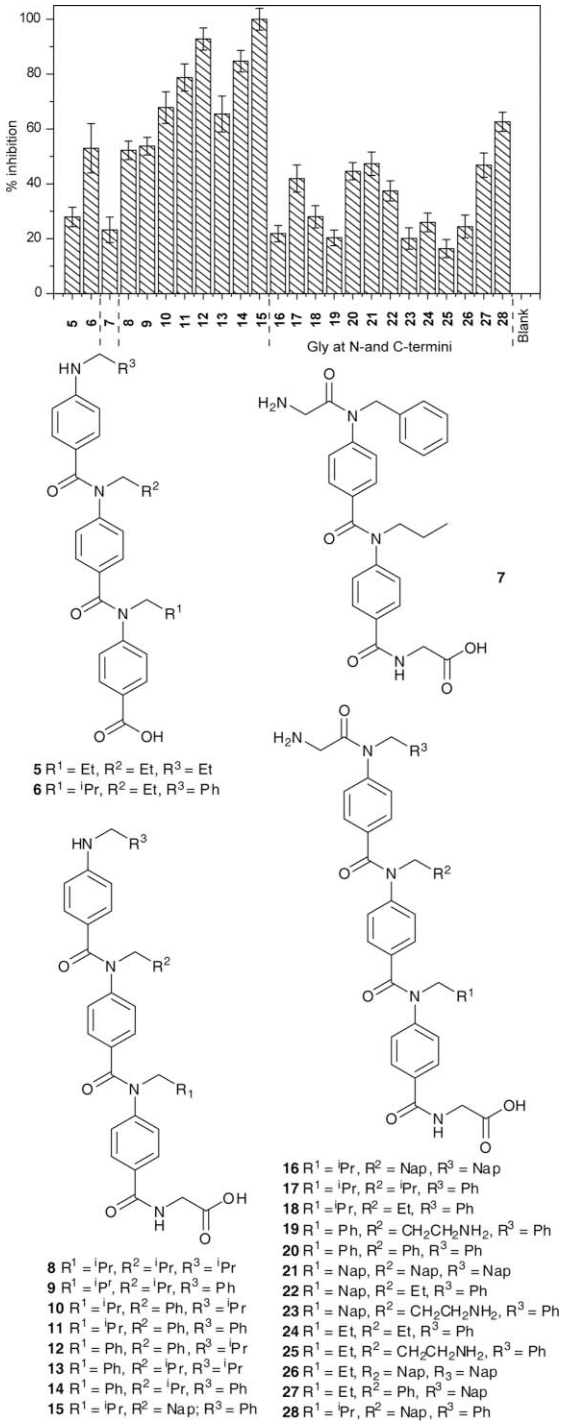

Fig. 2 Single point fluorescence anisotropy response for compounds **5–28** when tested for competitive inhibition of the p53–hDM2 interaction. ($p53_{15\text{-}29}$Flu 54 nM, *h*DM2 50 nM, 40 mM sodium phosphate, pH 7.4, 200 mM NaCl and 0.02 mg ml^{-1} of bovine serum albumin).

Table 1 IC_{50} values determined by fluorescence anisotropy competition assay[a]

Compound	IC_{50}/μM
$p53_{15\text{-}31Flu}$	0.074 (± 0.004)[b]
$p53_{15\text{-}31}$	1.2 (± 0.04)
7	> 50 (± 10)
11	3.8 (± 0.8)
12	4.1 (± 0.9)
14	3.3 (± 0.9)
15	2.8 (± 0.8)

[a] Conditions as indicated in Fig. 2. [b] K_d.

IC_{50} values for the most potent inhibitors of the p53–*h*DM2 interaction were subsequently determined (Table 1). Compound **15** was observed to inhibit the interaction with IC_{50} = 2.8 μM, which is comparable to the native peptide IC_{50} = 1.2 μM. Compounds **11**, **12** and **14** gave IC_{50} values of 3.8, 4.1 and 3.3 μM, respectively (see ESI†). We also tested compound **7** with only two side chains—as expected poor inhibition was observed IC_{50} > 50 μM. As was the case in our recently reported article on *O*-alkylated aromatic oligoamides,[48,60] we were unable to use this data to extract a K_d value because the tracer compound ($p53_{15\text{-}29Flu}$) interacts with both the helix mimetics and the positive control (unlabelled p53 peptide) resulting in a more complicated equilibrium. A comparison with published affinities of p53–*h*DM2 inhibitors[15,16,18] is also difficult to make given that various different assays have been used. The compounds are however, equipotent to (i) the native peptide and more significantly (ii) the rigid oligobenzamides we recently described,[48] which is impressive given the preferred *cis*-geometry of the amides in the unbound ligand.

Structural studies

We performed ^{1}H–^{15}N HSQC perturbation shift experiments[62] to establish that the α-helix mimetics bind to *h*DM2 at the peptide binding cleft. Distinct complexation induced shifts were observed upon addition of compound **11** (used because of superior solubility) to the apo form of the protein (see ESI†). Although these were smaller in magnitude, they were similar in nature to those observed upon addition of the p53 peptide. When mapped onto the crystal structure of the *h*DM2–p53 structure (1YCR),[8] the shifts clearly show that throughout the protein, structural changes occur upon formation of the hydrophobic cleft that accommodates either p53 or compound **11** (Fig. 3). The experiment also lends further support to the notion that the helix mimetic indeed adopts an extended conformation to bind to the protein as shifts are observed for residues at either end of the helix binding cleft on *h*DM2.

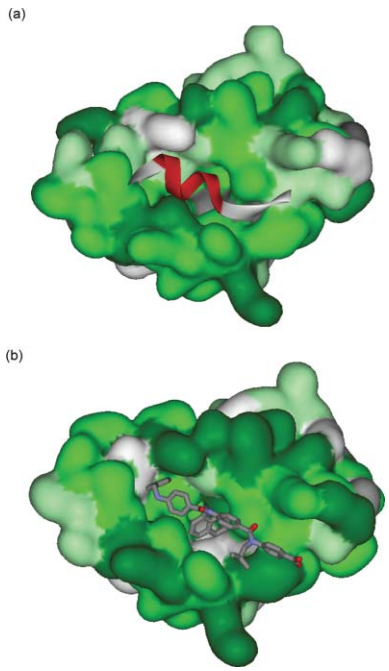

Fig. 3 ^{1}H–^{15}N HSQC chemical shift perturbation mapping onto the crystal structure of p53–*h*DM2 (a) p53 peptide (b) helix mimetic **11**—a model of the proteomimetic has been manually docked into the protein to indicate where we perceive binding to occur (regions that experience: large shifts are shown in dark green, medium shifts in green and weak shifts in light green, unassigned peaks are highlighted in grey).

Conclusions

In conclusion, we have reported the design and solid-phase library synthesis of the simplest oligoamide α-helix mimetic scaffold yet described and shown that such compounds act as potent inhibitors of the p53–*h*DM2 interaction through interaction with *h*DM2. The ability to rapidly construct focused libraries or much larger libraries for high throughput screening using SPS offers immense new opportunities for the discovery of inhibitors of protein–protein interactions. Our ongoing studies will build upon these preliminary results and are focused towards gaining a greater understanding of the structural and thermodynamic basis of this inhibition, improving potency/selectivity and targeting other protein–protein interactions *in vitro* and *ex vivo*.

Experimental

General considerations

All reagents were obtained from Aldrich, Alfa Aesar, Acros or Fluka and used without further purification. All solvents used were HPLC grade. Dry solvents were distilled from sodium/benzophenone (THF, Et_2O) or calcium hydride (CH_2Cl_2) immediately prior to use. *N*-methylimidazole was distilled from calcium hydride. Analytical TLC was performed using 0.2 mm silica gel 60 F_{254} pre-coated aluminium sheets (Merck) and visualised using UV irradiation or, in the case of amine intermediates, by staining with a ninhydrin solution. Flash column chromatography was carried out on silica gel 60 (35 to 70 micron particles, FluoroChem). Solvent ratios are described where appropriate. Solvents were removed under reduced pressure using a Buchi rotary evaporator at diaphragm pump pressure. Samples were freed of remaining traces of solvents under high vacuum. ^{1}H and ^{13}C NMR spectra were measured on a Bruker DPX300 or a Bruker Avance 500 spectrometer using an internal deuterium lock. Chemical shifts are reported in parts per million (ppm) downfield from TMS in δ units and coupling constants are given in hertz (Hz). Coupling constants are reported to the nearest 0.1 Hz. TMS is defined as 0 ppm for ^{1}H NMR spectra and the centre line of the triplet of $CDCl_3$ was defined as 77.10 ppm for ^{13}C NMR spectra. When describing ^{1}H NMR data the following abbreviations are used; s = singlet, d = doublet, t = triplet, q = quartet, m = multiplet app = apparent. Melting points were determined using a Griffin D5 variable temperature apparatus and are uncorrected. Microanalyses were obtained on a Carlo Erba Elemental Analyser MOD 1106 instrument, found composition is reported to the nearest 0.05%. Infrared spectra were recorded on a Perkin-Elmer FTIR spectrometer and samples analysed as solids (unless stated). Mass spectra (HRMS) were recorded in house using a Micromass GCT Premier, using electron impact ionisation (EI) or a Bruker Daltonics micrOTOF, using electron spray ionisation (ES). LC-MS experiments were run on a Waters Micromass ZQ spectrometer, samples ionised by electrospray and analysed by a time-of-flight mass spectrometer, or a Bruker Daltronics HCTUltra™ series spectrometer, samples ionised by electrospray. All experiments were run through a C18 column on an acetonitrile–water gradient (typically 0–95% acetonitrile over 3 min). The synthesis of compounds **5** and **6** was described earlier.[53] A representative example of each synthetic procedure is provided with all examples described in the ESI.†

Reductive amination

To a stirred solution of primary aniline (1 eq.) and aldehyde (≥1 eq.) in methanol, under an atmosphere of nitrogen, was added borane-picoline (small excess). The reaction mixture was stirred at 35 °C for 12–36 h, until TLC indicated reaction completion. Concentration and direct purification by column chromatography gave the target material which was dried under vacuum and fully characterised.

(Note: borane-picoline—a white solid with greater stability than borane-pyridine can also be used for this reaction.)

4-(Propylamino)benzoic acid 2a

4-Aminobenzoic acid (2.50 g, 18.2 mmol), propionaldehyde (1.70 mL, 23.6 mmol) and picoline-borane complex (2.00 g, 18.7 mmol) were stirred at room temperature in methanol (25 mL) for 14 h. The reaction mixture was then concentrated and triturated with the minimum amount of hot chloroform then allowed to cool. The resultant solid was crystallised from chloroform to yield target material (2.28 g, 12.7 mmol, 70%) as a pale cream solid; m.p. 163–164 °C; R_F 0.19 (10% MeOH in CH_2Cl_2); δ_H (300 MHz, MeOD) 0.89 (t, 3H, J = 7.4 Hz, $CH_3CH_2CH_2$), 1.53 (m, 2H, $CH_3CH_2CH_2$), 2.98 (t, 2H, J = 7.2 Hz, $CH_3CH_2CH_2$), 6.46 (d, 2H, J = 8.9 Hz, ArH), 7.66 (d, 2H, J = 8.9 Hz, ArH); δ_C (75 MHz, MeOD) 12.2, 23.6, 46.1, 112.3, 118.1, 133.1, 155.0, 171.2; ν_{max}/cm^{-1} (solid state) = ~3000 (COOH), 1657 (CO); ESI-HRMS found m/z 180.1021 $[M+H]^+$ $C_{10}H_{14}NO_2$ requires 180.1019.

4-((((9*H*-Fluoren-9-yl)methoxy)carbonyl)(propyl)amino)benzoic acid 3a

To a refluxing solution of 4-(propylamino)benzoic acid (500 mg, 2.8 mmol) in chloroform (15 mL) was added dropwise a solution of Fmoc chloride (865 mg, 3.3 mmol) in chloroform (10 mL) over a period of 1 h. The reaction mixture was then stirred at reflux for an additional 16 h. Column chromatography (*Stationary Phase*: Silica, 90 g; *Mobile Phase*: CH_2Cl_2 to 15% EtOAc in CH_2Cl_2) yielded target material (939 mg, 2.3 mmol, 88%) as an amorphous solid; (Found: C, 74.50; H, 5.85; N, 3.45; requires: C, 74.79; H, 5.77; N, 3.49); R_F 0.36 (15% EtOAc in CH_2Cl_2); δ_H (300 MHz, $CDCl_3$) 0.81 (t, 3H, J = 7.4 Hz, $CH_3CH_2CH_2$), 1.46 (m, 2H, $CH_3CH_2CH_2$), 3.58 (t, 2H, J = 7.4 Hz, $CH_3CH_2CH_2$), 4.13 (t, 1H, J = 6.0 Hz, $CHCH_2$), 4.52 (d, 2H, J = 6.1 Hz, $CHCH_2$), 7.16-7.39 (m, 8H, ArH), 7.71 (d, 2H, J = 7.5 Hz, ArH), 8.04 (d, 2H, J = 8.6 Hz, ArH); δ_C (75 MHz, $CDCl_3$) 11.0, 21.5, 47.2, 51.7, 64.2, 67.3, 119.9, 120.1, 124.8, 126.8, 127.0, 127.7, 131.0, 141.4, 143.7, 146.8, 154.9, 170.9; ν_{max}/cm^{-1} (solid state) = ~3000 (COOH), 1720, 1673 (CO); ESI-MS m/z 402 $[M+H]^+$.

Solid phase synthesis experimental

25–30 mg of Fmoc-Gly-Wang resin (0.4–0.8 mmol g^{-1}, 100-200 mesh; carrier: polystyrene, crosslinked with 1% DVB) from Fluka, was used throughout. All solvents used were HPLC grade. Anhydrous chloroform was freshly distilled over calcium chloride prior to every use. 1-Chloro-*N*,*N*,2-trimethyl-1-propenylamine (Ghosez reagent) was purchased from Sigma-Aldrich and used as a 10% stock solution in anhydrous CH_2Cl_2. Freshly distilled methyl imidazole was used throughout. The reactions were all carried out in 1.5 mL 'Extract-Clean' polypropylene reservoirs fitted with 20 μm polyethylene frits, both available from Alltech. For each coupling reaction, 10 equivalents of fully protected monomer, 9 equivalents of Ghosez reagent (~270 μL of 10% stock solution) and 20 equivalents of methyl imidazole were used. The total volume in each reservoir was 750 μL.

Coupling

Prior to the reaction, each fully protected monomer was dissolved in anhydrous chloroform and concentrated before final drying under high vacuum. The monomer was then dissolved in anhydrous chloroform (~450 μL) and Ghosez reagent added. This mixture was then allowed to incubate, prior to addition to the resin, for 3 h at room temperature in a sealed, flame dried flask. (Due to issues with solubility, it was necessary to incubate the Fmoc-glycine-4-naphthylaminobenzoic acid monomer with Ghosez in anhydrous chloroform reagent at 50 °C for 3 h.)

After three hours incubation, methyl imidazole was added and the reaction mixture added to the deprotected resin that had been washed several times with anhydrous chloroform. Each coupling reaction was allowed to stir for approximately 20 h.

Fmoc deprotection

After each coupling reaction, the contents of the reservoir were drained and the resin washed three times with CH_2Cl_2 and three times with DMF (750 μL each). Following the final DMF wash, the resin was then consecutively washed with 25% piperidine in DMF then neat DMF four times (750 μL each). Finally, the deprotected resin was washed twice with CH_2Cl_2 (750 μL each).

Cleavage and recrystallisation

Each reservoir was filled with neat TFA (750 μL) and allowed to stir for 2 h. After 2 h the contents of the reservoir were collected, concentrated and the target compound purified as detailed below

2-(4-(*N*-Isobutyl-4-(*N*-isobutyl-4-(isobutylamino)benzamido)-benzamido)benzamido)acetic acid 8. Purified by column chromatography (*Stationary Phase*: Silica, 15 g; *Mobile Phase*: CH_2Cl_2 to 15% MeOH in CH_2Cl_2). Precipitated from $CHCl_3$–hexane. Isolated yield: 4 mg. δ_H (500 MHz, MeOD) 0.78 (d, 6H, J = 6.7 Hz, $(CH_3)_2$), 0.86 (d, 12H, J = 6.8 Hz, 2 × $(CH_3)_2$), 1.76 (m, 3H, 3 × CH), 2.79 (d, 2H, J = 6.8 Hz, CH_2), 3.61 (d, 2H, J = 6.9 Hz, CH_2), 3.74 (d, 2H, J = 7.0 Hz, CH_2), 3.99 (s, 2H, CH_2), 6.21 (d, 2H, J = 9.6 Hz, ArH), 6.83 (d, 2H, J = 8.5 Hz, ArH), 6.88 (d, 2H, J = 8.8 Hz, ArH), 7.12 (m, 4H, ArH), 7.68 (d, 2H, J = 8.7 Hz, ArH); ν_{max}/cm^{-1} (solid state) = 3359 (COOH), 1734, 1635, 1602 (CO); ESI-HRMS found m/z 601.3380 $[M+H]^+$ $C_{35}H_{45}N_4O_5$ requires 601.3384.

Expression and purification of *h*DM2 17-126 L33E. *h*DM2 (17–126) construct was kindly provided by John Robinson at University of Zürich. The pET14b plasmid (Novagen) containing cDNA encoding *h*DM2 residues Ser17 to Asn126, with a single mutation L33E, was introduced into *E. coli* BL21 (DE3) GOLD. Protein production in 2xYT medium with ampicillin (100 μg mL^{-1}) was induced with IPTG (0.8 mM) when the optical density of the cell suspension reached OD_{600} = 0.8. Induced cells were grown at 18 °C for 12 h and harvested by centrifugation at 6000 rpm for 10 min. Cells were resuspended in buffer A (20 mM Tris, 500 mM NaCl, pH 7.9) with 0.1% Triton X-100, disrupted by 20 kPsi on a Cell Disruptor (Constant System Ltd.) and sonicated in the presence of DNaseI, 1 U mL^{-1} (EPICENTRE biotechnologies) and 5 mM $MgCl_2$. Cell lysate was centrifuged at 17 000 rpm for 30 min. Supernatant was loaded onto a Ni^{2+}-nitriloacetic acid (NTA) column equilibrated with buffer A. His_6-tagged *h*DM2

recombinant fragment was washed with 50 mL buffer A and buffer A with 60 mM imidazole added. The protein was eluted with 120 mM and 300 mM imidazole and the column was washed with 1 M imidazole in buffer A. Fractions containing protein were detected by 16% SDS-PAGE and concentrated to 5 mL then loaded onto a Superdex™ 75 column and washer with buffer B (25 mM Tris, 150 mM NaCl, 5% glycerol, 1 mM EDTA, 1 mM DTT, pH 7.3). The purified protein was concentrated to a final concentration of 83 μM and stored at −70 °C until use.

Expression and purification of ^{15}N labelled *h*DM2 17-126 L33E. *E. coli* BL21 (DE3) GOLD transformed with pET14b/hDM2 (17-126) L33E were grown in minimal HCDM1 media (KH_2PO_4 10 g l^{-1}, K_2HPO_4 10 g l^{-1}, Na_2HPO_4 7.2 g l^{-1}, $^{15}NH_4Cl$, 1.1 g l^{-1}; with added $MgCl_2$ 0.19 g l^{-1} and Glucose 4 g l^{-1} after autoclaving). Protein was purified as described above.

Fluorescence polarisation displacement assay

$p53_{15\text{-}31}$ transactivation domain peptide (Ac-SQETFSDLWKLLPENNVC-NH_2) (p53) and its fluorescein-labelled analogue (Ac-SQETFSDLWKLLPENNVC(Flu)-NH_2) ($p53_{15\text{-}31Flu}$, p53*) were purchased from Peptide Protein Research Ltd. Fluorescence anisotropy assays were performed in 96 well plates. All experiments were performed in 40 mM phosphate buffer at pH 7.42, containing 200 mM NaCl and 0.02 mg mL^{-1} bovine serum albumin (BSA). A series of blank experiments were run to ensure that *h*DM2, p53 and BSA, did not contribute to the overall fluorescence of the well. The serial dilutions of p53 and *h*DM2 in buffer (both with and without BSA) correspondingly gave no significant fluorescence. In all experiments the G factor, or ratio between the efficiency of the S(ame) and P(erpendicular) channels, was set to 1.

Determination of the binding of p53* to *h*DM2

The procedure followed was described in our previous paper on *O*-alkylated aromatic oligoamides.[48] Briefly: *h*DM2 was serially diluted (41.5 pM - 4.15 μM) into a solution of p53* (54.5 nM) (40 mM Sodium phosphate buffer pH 7.54, 200 mM NaCl, 0.02 mg ml^{-1} of bovine serum albumin)—the total volume of each well was 160 μL. Each experiment was run in triplicate and the fluorescence polarisation measured using a Perkin Elmer EnVision™ 2103 MultiLabel plate reader, with excitation at 480 nm and emission at 535 nm (5 nM bandwidth) and the intensity (eqn (1)) was calculated for each point. This was used to calculate anisotropy (eqn (2)) and plotted to a sigmoidal fit in origin 7 to determine the minimum and maximum anisotropies (r_{min} and r_{max}). Using eqn (3), the data for the anisotropy was converted to fraction bound and multiplied by the $p53_{15\text{-}31Flu}$ concentration then fitted in origin 7 (eqn (4)) to give the dissociation constant K_d = 74 ± 4 nM.

$$I = (2PG) + S \tag{1}$$

$$r = \frac{S - PG}{I} \tag{2}$$

$$L_b = \frac{(r - r_{min})}{(\lambda(r_{max} - r) + r - r_{min})} \tag{3}$$

$$y = \frac{\{(k_1 + x + [FL]) - \sqrt{\{(k_1 + x + [FL])^2 - 4x[FL]\}}}{2} \tag{4}$$

r = anisotropy, I = total intensity, P = perpendicular intensity, S = parallel intensity, L_b = fraction ligand bound, $\lambda = I_{bound}/I_{unbound}$ = 1, [FL] = concentration of fluorescent ligand (*i.e.* $p53_{15\text{-}31Flu}$), $k_1 = K_d$, $y = L_b$* $p53_{15\text{-}31Flu}$ and x = [added titrant], G is an instrument factor set to 1.

Single point fluorescence anisotropy screening for inhibition of p53–*h*DM2 interaction

A one point assay was carried out on 24 compounds at a fixed concentration of inhibitor (10 μM), p53* (54.5 nM) and *h*DM2 (41.5 nM) in phosphate buffer. Each compound was assessed in triplicate and left to equilibrate overnight in the dark. No protein denaturation was observed over time, as evidenced by the control/blank experiment lacking ligand in which p53* remains fully bound to the protein. The anisotropy values were then determined and used to calculate p53* fraction bound (L_b) as above and then the percentage inhibition was calculated using these values.

Competition assay

Ligand (typically 2.5 nM–250 μM) was serially diluted into a solution of p53* (54.5 nM) and *h*DM2 (41.5 nM) in phosphate buffer containing BSA—the total volume of each well was 160 μL. The total fluorescence intensity and anisotropy were both calculated. The anisotropy was then plotted against ligand concentration in Origin 7 and fit to a dose response model (eqn (5)) to extract an IC_{50} value.

$$y = r_{min} + \frac{r_{max} - r_{min}}{1 + 10^{(x - \log x_o)}} \tag{5}$$

HSQC perturbation shift analysis

All HSQC experiments were performed on a Varian Inova spectrometer at 600 MHz in 60 mM sodium phosphate and 60 mM sodium acetate buffer at pH 7.3 at a constant temperature of 25 °C. There was 10% D_2O present to allow for a lock signal. Shigemi tubes were used and the volume of the solution was 300 μL. A gradient filtered pulse sequence was used and the data was phased using NMRpipe[63] and visualised using NMRview 5.22[64] The HSQC shift mapping was done on Accelerysis Weblab Viewer by separating the difference in chemical shift to four categories (Strong, Medium, Weak, and None) and colouring the residues accordingly with darker colours representing the stronger shifts. Grey was chosen for residues that were unassigned. The difference in chemical shift was calculated (eqn (6)) where $\Delta\delta_{overall}$ is the overall change in chemical shift $\Delta\delta_N$ is the change in the nitrogen dimension and $\Delta\delta_H$ is the change in the hydrogen dimension. The change in hydrogen dimension is scaled by the ratio of the magnetogyric radius of Nitrogen and Hydrogen to account for the larger chemical shift range of Nitrogen.[65] Each HSQC was obtained from 300 μL of labelled *h*DM2 (0.125 mM). To obtain the spectra with a mix of compounds a stock solution of either the mimetic or p53 was added in DMSO, ensuring that the protein would be saturated and the compound would still be soluble. In

the case of the mimetic the final concentration was 250 μM and for p53 it was 200 μM. In each case the amount of DMSO added was less than 5% of the total volume of the protein. Fig. ESI 2a and b show the HSQC spectra in the absence and presence of p53 and mimetic respectively whilst Fig. ESI 3 illustrates the shift changes by residue.† Large shifts were defined as greater than 0.3 ppm, medium as between 0.3 to 0.09 and weak shifts those below 0.09.

$$\Delta\delta_{overall} = \sqrt{\left(\Delta\delta_N\right)^2 + \left(\frac{\gamma_H}{\gamma_N}\right)^2 \left(\Delta\delta_H\right)^2} \quad (6)$$

To compare the changes seen in the HSQC we also mapped the shifts in α-carbons between the NMR structure of the apo protein (PDBID: 1Z1M) with both the crystal structures of bound p53 (1YCR) and nutlin (1RV1). The structures were overlaid with the least squares function in COOT[66] and the distances between each carbon were calculated (eqn (7))

$$\Delta_{Overall} = \sqrt{\Delta_x^2 \times \Delta_y^2 \times \Delta_z^2} \quad (7)$$

The positional changes were separated into three groups (Large, Medium, and Small) and mapped to the structure of *h*DM2 in a similar manner as for the HSQC shifts.

Acknowledgements

This work was supported by the Engineering and Physical Sciences Research Council [EP/D077842/1 and EP/G022569/1] and The European Research Council [240342]

Notes and references

1 T. Berg, *Angew. Chem., Int. Ed.*, 2003, **42**, 2462–2481.
2 H. Yin and A. D. Hamilton, *Angew. Chem., Int. Ed.*, 2005, **44**, 4130–4163.
3 J. A. Wells and C. L. McLendon, *Nature*, 2007, **450**, 1001–1009.
4 A. J. Wilson, *Chem. Soc. Rev.*, 2009, **38**, 3289–3300.
5 J. M. Davis, L. K. Tsou and A. D. Hamilton, *Chem. Soc. Rev.*, 2007, **36**, 326–334.
6 M. Sattler, H. Liang, D. Nettesheim, R. P. Meadows, J. E. Harlan, M. Eberstadt, H. S. Yoon, S. B. Shuker, B. S. Chang, A. J. Minn, C. B. Thompson and S. W. Fesik, *Science*, 1997, **275**, 983–986.
7 G. Lessene, P. E. Czabotar and P. M. Colman, *Nat. Rev. Drug Discovery*, 2008, **7**, 989–1000.
8 P. H. Kussie, S. Gorina, V. Marechal, B. Elenbaas, J. Moreau, A. J. Levine and N. P. Pavletich, *Science*, 1996, **274**, 948–953.
9 S. Patel and M. R. Player, *Expert Opin. Invest. Drugs*, 2008, **17**, 1865–1882.
10 J. K. Murray and S. H. Gellman, *Peptide Science*, 2007, **88**, 657–686.
11 T. Oltersdorf, S. W. Elmore, A. R. Shoemaker, R. C. Armstrong, D. J. Augeri, B. A. Belli, M. Bruncko, T. L. Deckwerth, J. Dinges, P. J. Hajduk, M. K. Joseph, S. Kitada, S. J. Korsmeyer, A. R. Kunzer, A. Letai, C. Li, M. J. Mitten, D. G. Nettesheim, S.-C. Ng, P. M. Nimmer, J. M. O'Connor, A. Oleksijew, A. M. Petros, J. C. Reed, W. Shen, S. K. Tahir, C. B. Thompson, K. J. Tomaselli, B. Wang, M. D. Wendt, H. Zhang, S. W. Fesik and S. H. Rosenberg, *Nature*, 2005, **435**, 677–681.
12 A. Degterev, A. Lugovskoy, M. Cardone, B. Mulley, G. Wagner, T. Mitchison and J. Y. Yuan, *Nat. Cell Biol.*, 2001, **3**, 173–182.
13 J.-L. Wang, D. Liu, Z.-J. Zhang, S. Shan, X. Han, S. M. Srinivasula, C. M. Croce and E. S. Alnemri, *Proc. Natl. Acad. Sci. U. S. A.*, 2000, **97**, 7124–7129.
14 M. Nguyen, R. C. Marcellus, A. Roulston, M. Watson, L. Serfass, S. R. Murthy-Madiraju, D. Goulet, J. Viallet, L. Belec, X. Billot, S. Acoca, E. Purisima, A. Wiegmans, L. Cluse, R. W. Johnstone, P. Beauparlant and G. C. Shore, *Proc. Natl. Acad. Sci. U. S. A.*, 2007, **104**, 19512–19517.
15 L. T. Vassilev, B. T. Vu, B. Graves, D. Carvajal, F. Podlaski, Z. Filipovic, N. Kong, U. Kammlott, C. Lukacs, C. Klein, N. Fotouhi and E. A. Liu, *Science*, 2004, **303**, 844–848.
16 B. L. Grasberger, T. Lu, C. Schubert, D. J. Parks, T. E. Carver, H. K. Koblish, M. D. Cummings, L. V. LaFrance, K. L. Milkiewicz, R. R. Calvo, D. Maguire, J. Lattanze, C. F. Franks, S. Zhao, K. Ramachandren, G. R. Bylebyl, M. Zhang, C. L. Manthey, E. C. Petrella, M. W. Pantoliano, I. C. Deckman, J. C. Spurlino, A. C. Maroney, B. E. Tomczuk, C. J. Molloy and R. F. Bone, *J. Med. Chem.*, 2005, **48**, 909–912.
17 I. R. Hardcastle, S. U. Ahmed, H. Atkins, G. Farnie, B. T. Golding, R. J. Griffin, S. Guyenne, C. Hutton, P. Källblad, S. J. Kemp, M. S. Kitching, D. R. Newell, S. Norbedo, J. S. Northen, R. J. Reid, K. Saravanan, H. M. G. Willems and J. Lunec, *J. Med. Chem.*, 2006, **49**, 6209–6221.
18 S. Shangary, D. Qin, D. McEachern, M. Liu, R. S. Miller, S. Qiu, Z. Nikolovska-Coleska, K. Ding, G. Wang, J. Chen, D. Bernard, J. Zhang, Y. Lu, Q. Gu, R. B. Shah, K. J. Pienta, X. Ling, S. Kang, M. Guo, Y. Sun, D. Yang and S. Wang, *Proc. Natl. Acad. Sci. U. S. A.*, 2008, **105**, 3933–3938.
19 E. A. Harker, D. S. Daniels, D. A. Guarracino and A. Schepartz, *Bioorg. Med. Chem.*, 2009, **17**, 2038–2046.
20 O. M. Stephens, S. Kim, B. D. Welch, M. E. Hodsdon, M. S. Kay and A. Schepartz, *J. Am. Chem. Soc.*, 2005, **127**, 13126–12127.
21 J. A. Kritzer, J. D. Lear, M. E. Hodsdon and A. Schepartz, *J. Am. Chem. Soc.*, 2004, **126**, 9468–9469.
22 J. D. Sadowsky, W. D. Fairlie, E. B. Hadley, H.-S. Lee, N. Umezawa, Z. Nikolovska-Coleska, S. Wang, D. C. S. Huang, Y. Tomita and S. H. Gellman, *J. Am. Chem. Soc.*, 2007, **129**, 139–154.
23 W. S. Horne, M. D. Boersma, M. A. Windsor and S. H. Gellman, *Angew. Chem., Int. Ed.*, 2008, **47**, 2853–2856.
24 E. F. Lee, J. D. Sadowsky, B. J. Smith, P. E. Czabotar, K. J. Peterson-Kaufman, P. M. Colman, S. H. Gellman and W. D. Fairlie, *Angew. Chem., Int. Ed.*, 2009, **48**, 4318–4322.
25 T. Hara, S. R. Durell, M. C. Myers and D. H. Appella, *J. Am. Chem. Soc.*, 2006, **128**, 1995–2004.
26 C. M. Goodman, S. Choi, S. Shandler and W. F. DeGrado, *Nat. Chem. Biol.*, 2007, **3**, 252–262.
27 R. Fasan, R. L. A. Dias, K. Moehle, O. Zerbe, D. Obrecht, P. R. E. Mittl, M. G. Grüttner and J. A. Robinson, *ChemBioChem*, 2006, **7**, 515–526.
28 S. Kneissl, E. J. Loveridge, C. Williams, M. P. Crump and R. K. Allemann, *ChemBioChem*, 2008, **9**, 3046–3054.
29 L. D. Walensky, A. L. Kung, I. Escher, T. J. Malia, S. Barbuto, R. D. Wright, G. Wagner, G. L. Verdine and S. J. Korsmeyer, *Science*, 2004, **305**, 1466–1470.
30 D. Wang, W. Liao and P. S. Arora, *Angew. Chem., Int. Ed.*, 2005, **44**, 6525–6529.
31 R. Hayashi, D. Wang, T. Hara, J. A. Iera, S. R. Durell and D. H. Appella, *Bioorg. Med. Chem.*, 2009, **17**, 7884–7893.
32 B. P. Orner, J. T. Ernst and A. D. Hamilton, *J. Am. Chem. Soc.*, 2001, **123**, 5382–5383.
33 O. Kutzki, H. S. Park, J. T. Ernst, B. P. Orner, H. Yin and A. D. Hamilton, *J. Am. Chem. Soc.*, 2002, **124**, 11838–11839.
34 J. T. Ernst, J. Becerril, H. S. Park, H. Yin and A. D. Hamilton, *Angew. Chem., Int. Ed.*, 2003, **42**, 535–550.
35 J. M. Davis, A. Truong and A. D. Hamilton, *Org. Lett.*, 2005, **7**, 5405.
36 H. Yin, G.-i. Lee, K. A. Sedey, J. M. Rodriguez, H.-G. Wang, S. M. Sebti and A. D. Hamilton, *J. Am. Chem. Soc.*, 2005, **127**, 5463–5468.
37 H. Yin, G.-I. Lee, K. A. Sedey, O. Kutzki, H. S. Park, B. P. Orner, J. T. Ernst, H.-G. Wang, S. M. Sebti and A. D. Hamilton, *J. Am. Chem. Soc.*, 2005, **127**, 10191–10196.
38 H. Yin, G.-I. Lee, H. S. Park, G. A. Payne, J. M. Rodriguez, S. M. Sebti and A. D. Hamilton, *Angew. Chem., Int. Ed.*, 2005, **44**, 2704–2707.
39 I. C. Kim and A. D. Hamilton, *Org. Lett.*, 2006, **8**, 1751–1754.
40 J. Becerril and A. D. Hamilton, *Angew. Chem., Int. Ed.*, 2007, **46**, 4471–4473.
41 S. M. Biros, L. Moisan, E. Mann, A. Carella, D. Zhai, J. C. Reid and J. Rebek, *Bioorg. Med. Chem. Lett.*, 2007, **17**, 4641–4645.
42 J. M. Rodriguez and A. D. Hamilton, *Angew. Chem., Int. Ed.*, 2007, **46**, 8614–8617.
43 I. Saraogi, C. D. Incarvito and A. D. Hamilton, *Angew. Chem., Int. Ed.*, 2008, **47**, 9691–9694.
44 P. Maity and B. König, *Org. Lett.*, 2008, **10**, 1473–1476.

45 J. M. Rodriguez, L. Nevola, N. T. Ross, G.-i. Lee and A. D. Hamilton, *ChemBioChem*, 2009, **10**, 829–833.
46 C. G. Cummings, N. T. Ross, W. P. Katt and A. D. Hamilton, *Org. Lett.*, 2009, **11**, 25–28.
47 A. Shaginian, L. R. Whitby, S. Hong, I. Hwang, B. Farooqi, M. Searcey, J. Chen, P. K. Vogt and D. L. Boger, *J. Am. Chem. Soc.*, 2009, **131**, 5564–5572.
48 J. P. Plante, T. Burnley, B. Malkova, M. E. Webb, S. L. Warriner, T. A. Edwards and A. J. Wilson, *Chem. Commun.*, 2009, 5091–5093.
49 T. Shahian, G. M. Lee, A. Lazic, L. A. Arnold, P. Velusamy, C. M. Roels, R. K. Guy and C. S. Craik, *Nat. Chem. Biol.*, 2009, **5**, 640–646.
50 F. Lu, S.-W. Chi, D.-H. Kim, K.-H. Han, I. D. Kuntz and R. K. Guy, *J. Comb. Chem.*, 2006, **8**, 315–325.
51 I. Huc, *Eur. J. Org. Chem.*, 2004, 17–29.
52 J. M. Rodriguez and A. D. Hamilton, *Angew. Chem. Int. Ed.*, 2007, **46**, 8614–8617.
53 F. Campbell, J. Plante, C. Carruthers, M. J. Hardie, T. J. Prior and A. J. Wilson, *Chem. Commun.*, 2007, 2240–2242.
54 F. Campbell and A. J. Wilson, *Tetrahedron Lett.*, 2009, **50**, 2236–2238.
55 S. Saito, Y. Toriumi, N. Tomioka and A. Itai, *J. Org. Chem.*, 1995, **60**, 4715–4720.
56 K. Yamaguchi, G. Matsumura, H. Kagechika, I. Azumaya, Y. Ito, A. Itai and K. Shudo, *J. Am. Chem. Soc.*, 1991, **113**, 5474–5475.
57 T. Heinz, D. M. Rudkevich and J. R. Jr., *Angew. Chem., Int. Ed.*, 1999, **38**, 1136–1139.
58 H. M. Konig, R. Abbel, D. Schollmeyer and A. F. M. Kilbinger, *Org. Lett.*, 2006, **8**, 1819–1822.
59 B. Blankemeyer-Menge, M. Nimtz and R. Frank, *Tetrahedron Lett.*, 1990, **31**, 1701–1704.
60 J. Plante, F. Campbell, B. Malkova, C. Kilner, S. L. Warriner and A. J. Wilson, *Org. Biomol. Chem.*, 2008, **6**, 138–146.
61 A. Devos, J. Remion, A. M. Frisque-Hesbain, A. Colens and L. Ghosez, *J. Chem. Soc., Chem. Commun.*, 1979, 1180–1181.
62 S. Uhrinova, D. Uhrin, H. Powers, K. Watt, D. Zheleva, P. Fischer, C. McInnes and P. N. Barlow, *J. Mol. Biol.*, 2005, **350**, 587–598.
63 F. Delaglio, S. Grzesiek, G. W. Vuister, G. Zhu, J. Pfeifer and A. Bax, *J. Biomol. NMR*, 1995, **6**, 277–293.
64 B. A. Johnson and R. A. Blevins, *J. Biomol. NMR*, 1994, **4**, 603–614.
65 T. A. Edwards, J. A. Butterwick, L. Zeng, Y. K. Gupta, X. Wang, R. P. Wharton, A. G. Palmer, III and A. K. Aggarwal, *J. Mol. Biol.*, 2006, **356**, 1065–1072.
66 P. Emsley and K. Cowtan, *Acta Crystallogr., Sect. D: Biol. Crystallogr.*, 2004, **60**, 2126–2132.